Iraqi Geological Journal

Journal homepage: https://www.igj-iraq.org

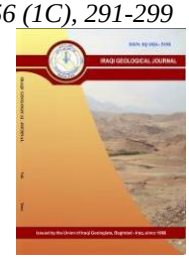

Evaluation of the Foundation Beds Liquidation by Using Soil Modeling for El-Burullus Power Plant Area, Kafr El-Sheikh, Egypt

Reda A. Warshal[1,*], Ahmed M. Saad[1] and Tarek I. Sabry[2]

[1] Geology Department, Faculty of Science, Al Azhar University, Cairo, Egypt

[2] High Institute for Engineering and Technology, Al-Behira, Egypt

* Correspondence: rwarshal72warshal@yahoo.com

Received:
8 December 2022

Accepted:
9 January 2023

Published:
31 March 2023

Abstract

In this study, the soil has been numerically modeled as the Mohr-Columb model because it is simple to capture essential features of soil behavior. Plaxis 2D software program has been used for modeling. The dynamic analyses depend on some data, such as grain size gradation for materials, stiffness and water level. This data has been used in the calculation process. Simple applications have been chosen to calculate the relations. The program computes entered data automatically. Earthquakes result in dynamic loading on soil which has a significant effect on the soil properties. The model is formed of five soil layers. Sands and mud deposits covered the area and Delta also. Some of the study results can be estimated by using the modeling method. The applied load value is 100 kN/m^2. The amplification factor (S %) to the soil in the study area is 108 % when soil is without the foundation load and 150 % when soil with foundation load. Thus, the soil is classified as type – D (Moderate) and no liquefaction is expected in the results, but subduction or landslide, so piling foundations are recommended within the area of study. As well, numerical modeling is recommended in several locations in Egypt to obtain suitable areas for the foundation constructions.

Keywords: Model; Finite element; Liquefaction; Plastic; Amplification factor

1. Introduction

The El-Burullus Power Plant area is considered a new project and it was chosen to be the study area. It is located within an area of approximately 1.050 Sq. km. The study area is defined by the following coordinates. Longitudes 30°48'7.27" and 30°49'3.66"E and latitudes 31°31' 23.84" and 31°32' 5.62"N. (Fig. 1). Different techniques are used to evaluate soil investigations, such as electrical resistivity imaging (Zghair et al., 2022), remote sensing technology (Shalal et al., 2022), and modeling program that was used in the present study. The geotechnical properties, including physical, engineering, chemical, and mineralogical characteristics are used to verify the quality of sediments (Qadir et al., 2022). This research gives us information about the foundations bed and determines the risk zone of the El-Burullus power plant area. There are six geomorphologic units along the coastal plain which are the nearshore zone, the shore, the coastal plain, the coastal sand dunes, the coastal lakes and the coastal sabkhas (Al Azab, 2006). He also concluded that, the studied sediment ranged between medium and fine sand. In the Abu Quir field, the Abu Madi Formation consists of evaporates intercalations and clastic of marine origin (El-Heiny and Enani, 1996). Northwest movement directions

DOI: 10.46717/igj.56.1C.20ms-2023-3-31

affecting on the west of Delta (Kebeasy, 1990). The study area is located in the northeastern corner of the African plate. The study of historical earthquakes is useful and constructive tool for understanding the undue consequences associated with ancient earthquakes. The distribution of the earthquake epicenters in Egypt is located along the main three trends. These trends are Fayum – Cairo – Pleseium trend, Red Sea, Gulf of Suez, Cairo – Alexandria trend and Gulf of Aqaba – Dead Sea trend.

The study area is characterized by the occurrence of micro, shallow, small and moderate earthquakes. The seismic activity depends on the geological structures. The majority of faults are steep normal faults and most of faults have a long age (Meneisy, 1990). Some of normal faults affected the study area (Brimich et al., 2011). Deposits of Quaternary and sand at the fault indicate young seismic effect (El-Shazly, et al., 1974; Kusky et al., 2011). The main target of the present work is subdivided into three main parts. The first part dealt with the geotechnical properties of the foundation bed. The second part dealt with the soil modeling. The third part dealt with geoenvironmental hazards.

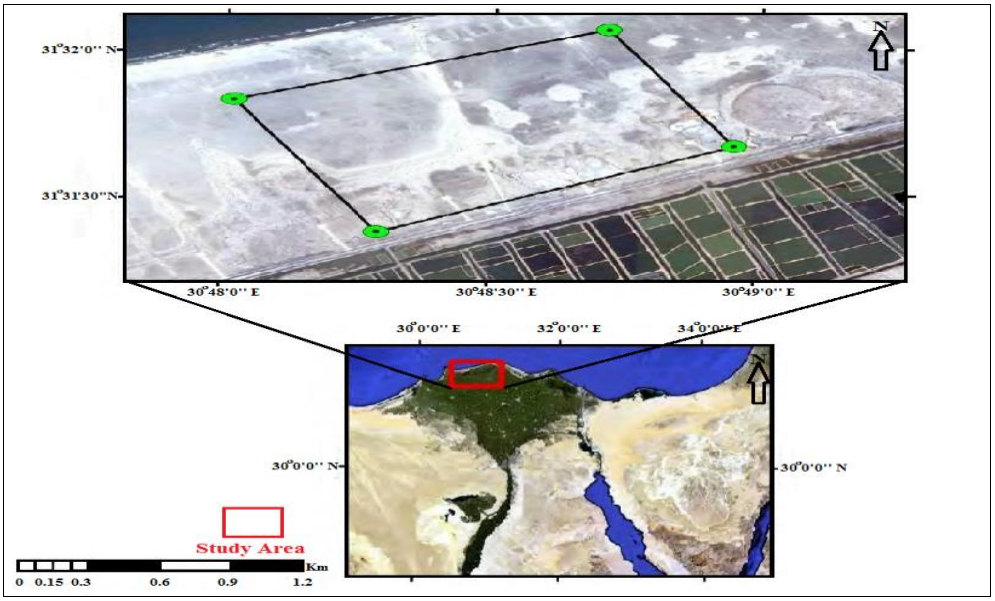

Fig. 1. Location map of the study area

2. Methodology

2.1. Soil Modeling

In this study, Plaxis 2D software has been used Version 8.6. Soil may be modeled at various degrees of accuracy by means of finite element technique. This program is used for analysis of stability and deformation. Plaxis program enables users to choose different soil models which is dependent on mechanical deformation behaviors of soil. Plaxis 2D Project (PLX) type is used for multi-bore holes. The water level was determined in this model. The raft foundation is modeled as elastoplastic plate element.

2.1.1. Input procedures

- General
  Model: Plain Strain
  Soil elements: 15-node triangular elements.
  Raft foundation elemen: Plate element.
- Geometry Model:
  Geometry Dimensions

Left: 0.00 m. Right: 100.00 m.
Bottom: 0.00 m. Top : 80.00 m.
Soil Stratigraphy
Five soil layers are classified as follows (from top to bottom) (Table 1).

Table 1. Soil types recorded at El-Burullus power plant area

Layer	Depth (m)		Layer Thickness (m)	Description
	From	To		
1	0.00	3.00	3.00	Dense sand poorly graded
2	3.00	6.00	3.00	Stiff clay with fine sand
3	6.00	9.00	3.00	Dense sand poorly graded
4	9.00	15.00	6.00	Stiff clay with fine sand
5	15.00	80.00	65.00	Dense sand poorly graded

Raft Foundation
Raft length= 10 m centered at top of the model.
The model length is 100 m and its depth is 80 m. The foundation length is 10 m and is located in the center of the model. The soil of El-Burullus Power Plant area from the foundation point of view is divided into two types: sandy soil and clay soil. The first type is classified as coarse grained sand which has a good load bearing capacities and good drainage qualities. The second type is classified as clay which has weak swelling properties, but a has high and very high plasticity index.

2.1.2. Material data sets and material model

Soil Layers: - Material Model: Mohr-Coulomb.
Material Type: Drained (Table 2).

Table 2. The parameters of different types of soil at El-Burullus power plant area

Layer	Symbol	Unit	1	2	3	4	5
Dry Density	γ_{dry}	kN/ m^3	15.70	13.86	16.29	14.27	13.86
Wet Density	γ_{wet}	kN/ m^3	16.64	20.79	17.10	20.12	14.55
Cohesion	C_{ref}	kN/ m2	1.00	49.00	1.00	23.00	1.00
Friction Angle	ϕ^o	Degrees	34.50	0.00	34.00	0.00	34.5
Dilatency Angle	ψ	Degrees	0.00	0.00	0.00	0.00	0.00
Young's Modulus	E_{ref}	kN/m^2	5000	4000	4500	6000	11000
Poisson's Ratio	ν	Unitless	0.36	0.44	0.35	0.45	0.30

2.1.3. Loading

- Vertical Loading on Raft
  In case of applying vertical load on raft, distributed load in the Y-direction
  = -100 kN/m^2 applied on the raft area.
- Earthquake 2.1.3.2.
  Input of horizontal displacement = 0.01 m.
  The vertical displacement = 0 m.
- Mesh Generation

Plaxis allowed mesh generation steps. The very fine coarseness of the finite element mesh is selected due to the expected large displacement gradients in the geometry. Fig. 2 presents the generated mesh and connectivities for the model. The model is formed of five soil layers.

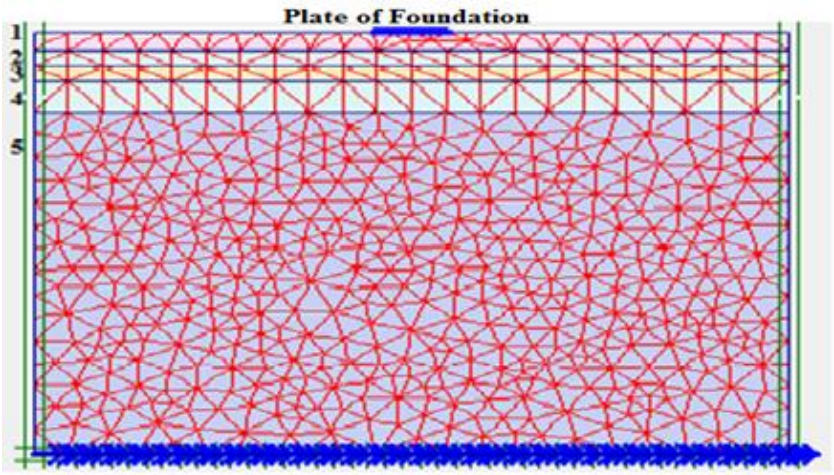

Fig. 2. Connectivities and meshing of the numerical model

- Primary Conditions

Phreatic level and groundwater head equal to 1.0 m below ground surface. Fig. 3 shows the extreme active pore water pressures.

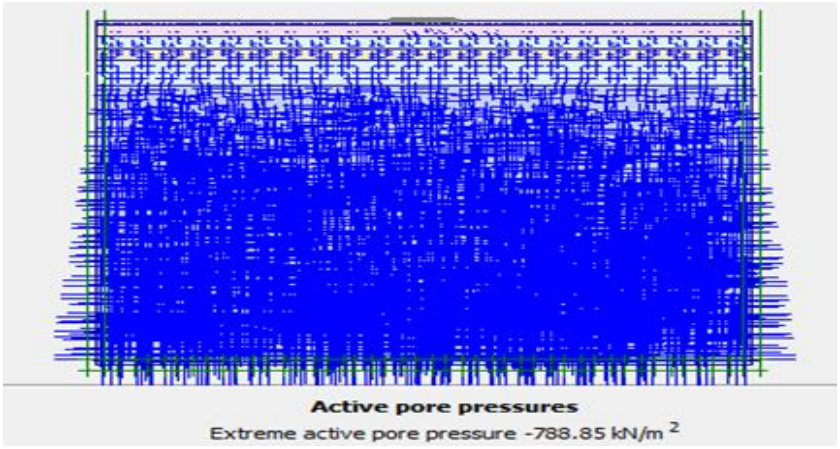

Fig. 3. Shows drawing for extreme active water pore pressuers

3. Results

3.1. Output

- Deformed Mesh.
- Displacements at all nodes, total, horizontal, and vertical (u_{total}, u_x , u_y).
- Strain at all nodes, total, horizontal, vertical, and shear strain (ε_{total}, ε_{xx} , ε_{yy}, γ_{xy}).
- Velocity at all nodes, total, horizontal, and vertical.
- Acceleration at all nodes, total, horizontal, and vertical.
- Vertical, horizontal, and shear stresses (σ'_{yy},σ'_{xx},σ'_{xy}) (Table 3).

Table 3. Shows the output results for the above two loading cases

Items	Symbol	Unit	Case (A)	Case (B)
Extreme total displacement	U_{total}	m	193×10^{-6}	232.10×10^{-3}
Extreme horizontal displacement	U_x	m	82.26×10^{-6}	35.97×10^{-3}
Extreme vertical displacement	U_y	m	175.13×10^{-6}	232.05×10^{-3}
Extreme principal strain	ε_{total}	%	51.53×10^{-3}	-12.33
Extreme horizontal strain	ε_{xx}	%	14.82×10^{-3}	2.67
Extreme vertical strain	ε_{yy}	%	-9.65×10^{-3}	-3.67
Extreme shear strain	γ_{xy}	%	-67.10×10^{-3}	-16.23
Extreme total velocity	V_{total}	m/sec	63.87×10^{-6}	1.46×10^{-3}
Extreme horizontal velocity	v_{xx}	m/sec	-46.52×10^{-6}	1.14×10^{-3}
Extreme vertical velocity	v_{yy}	m/sec	61.32×10^{-6}	1.33×10^{-3}
Extreme total acceleration	a_{total}	m/sec^2	1.48×10^{-3}	16.51×10^{-3}
Extreme horizontal acceleration	a_{xx}	m/sec^2	1.48×10^{-3}	-15.33×10^{-3}
Extreme vertical acceleration	a_{yy}	m/sec^2	1.23×10^{-3}	15.49×10^{-3}
Extreme vertical effective stress	σ'_{yy}	kN/m^2	-1.23×10^{3}	-1.24×10^{3}
Extreme horizontal effective stress	σ'_{xx}	kN/m^2	-531.16	-535.94
Extreme shear stress	σ'_{xy}	kN/m^2	-10.27	35.10

3.2. Amplification Factor of Soil

The amplification factor of soil is a very effective agent. The amplification factor can be calculated from relation No. 1 (Housner, 1952).

$$S = I_{Soil} / I_{Rock} \quad (1)$$

Table 4 shows the soil susceptibility to amplification according to Vs30 and others parameters.

Table 4. Classification of soil sense to amplification according to Building Seismic Safety Council, (1994)

Site Class	General Description	Definition (V_s30 = average shear-wave velocity in upper 30 m, m/sec)	Susceptibility Rating
A	Hard rock	$V_s30 > 1500$	Nil
B	rock	$760 < V_s30 < 1500$	Very Low
C	Very dense soil and soft rock	$360 < V_s30 < 760$; or $V_s30 > 760$ m/sec where >3m of soil over bedrock	Low
D	Stiff soils	$180 < V_s30 < 360$	Moderate
E	Soft soils	$V_s30 < 180$; or > 3m silt and clay with plasticity index > 20, moisture content > 40% and un drained shear strength < 25 kPa	High
F	Peats or highly organic clays	Peat thickness >3	Very High

The amplification factor of the study area is 108% in free case and this factor increases to 150% when load is found because of damping of load to ground motion, so that soil is classified according to Building Seismic Safety Council (1994) as type – D (Moderate), and the results are shown in Table 5.

Table 5. Percent of amplification factor (S%) to soil at the study area

Earthquake and load	I_{Soil} (ax. At A)	I_{Rock} (ax. At F)	S %	Ampl. Degree
Soil without foundation load	2.687	2.487	108	Moderate
Soil with foundation load	0.036	0.024	150	Moderate

4. Discussion

Calculation is made in two cases when subjected to an earthquake as follows:

Case(A): Raft foundation is subjected to an earthquake without applying static loads.

Case(B): Raft foundation is subjected to an earthquake after applying vertical distributed load = 100 KN/m^2.

4.1. Case (A)

Calculation Procedures (No external loads). Two calculation cases are summarized below:

Case I:This case is without load. Calculation type is called Plastic Analysis.

Case II: Earthquake effect takes place for time interval = 6 seconds. The calculation type is called Dynamic Analysis.

4.2. Case (B)

Calculation Procedures (Applying vertical loads). Calculation cases summarized below:

Step 1: Static load applied in this case. Calculation type is called Plastic Analysis.

Step 2: Applying vertical load = 100 kN/m^2 distributed downward on the raft. The calculation type is called Plastic Analysis.

Step 3: Earthquake effect takes place for time interval = 6 seconds. The calculation type is called Dynamic Analysis.

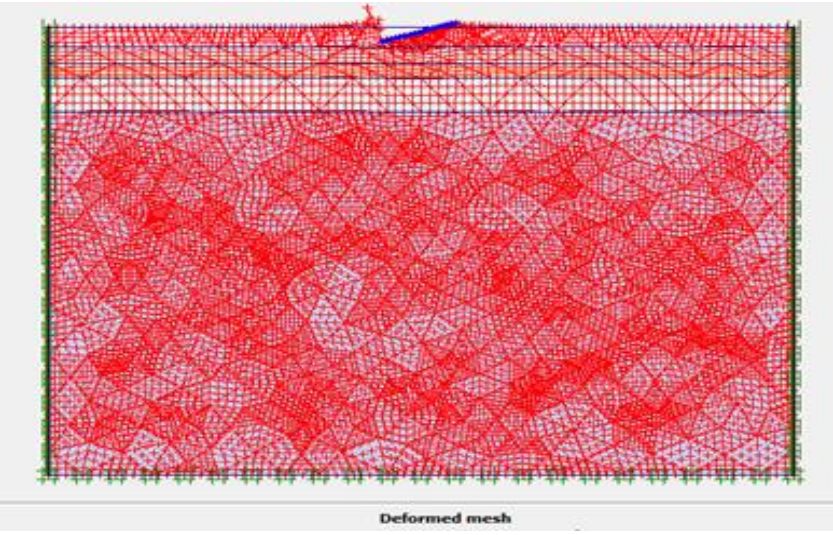

Fig. 4. Deformed mesh without load

Figures from 4 to 9 show some of output results for the above two loading cases of soil in El-Burullus power plant area. In Fig. 4, partial subsidence and mesh deformation in the top area of the model is observed without loading, while in Fig. 5 representes both subsidence in the foundation and mesh deformation are observed with loading.

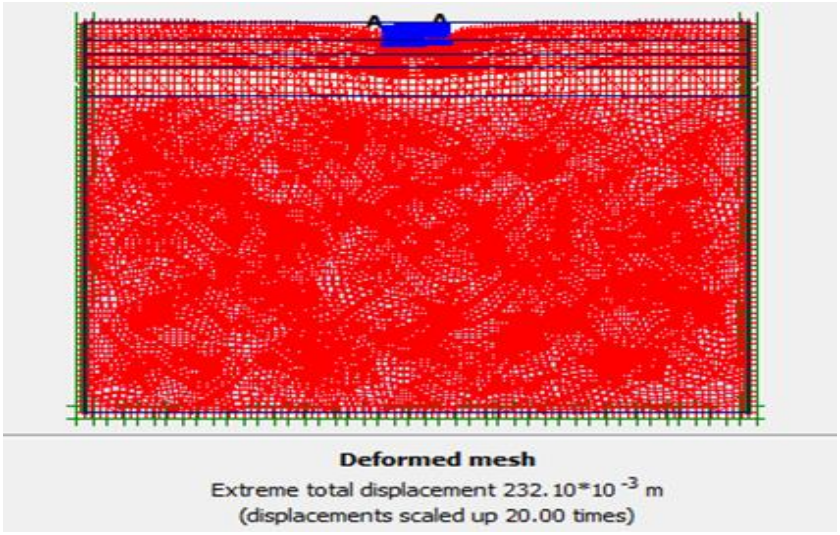

Fig. 5. Deformed mesh with load

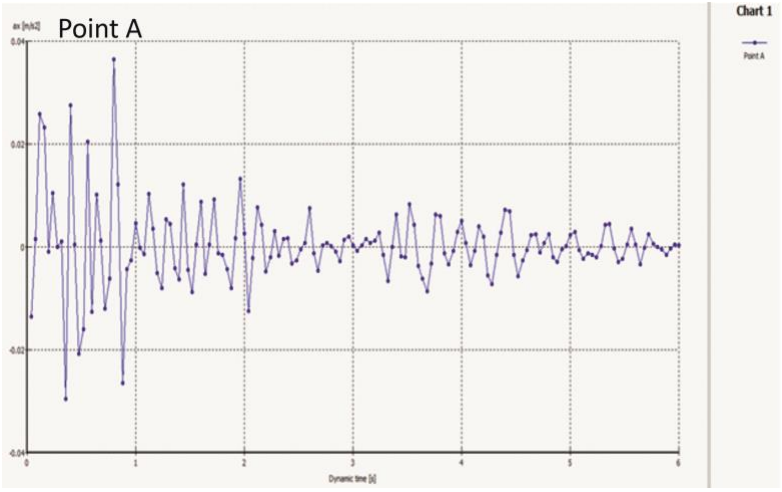

Fig. 6. Shows acceleration-time curve of soil without plate foundation load at surface (Point A)

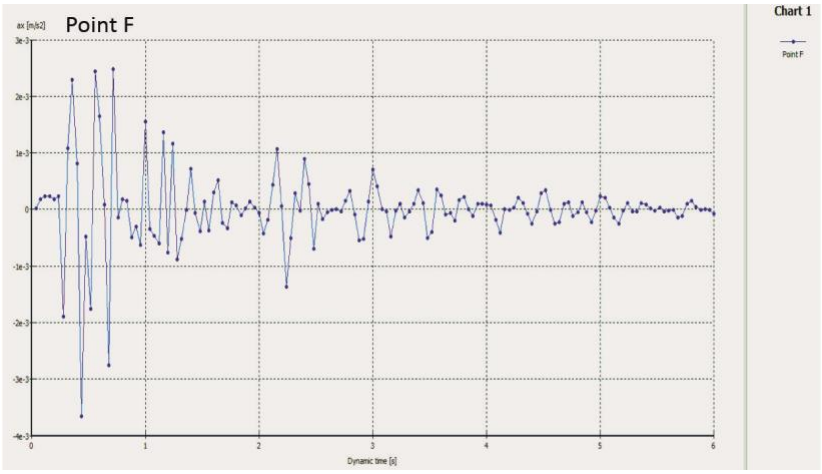

Fig. 7. Shows acceleration-time curve of soil without plate foundation load at bed rock (Point F)

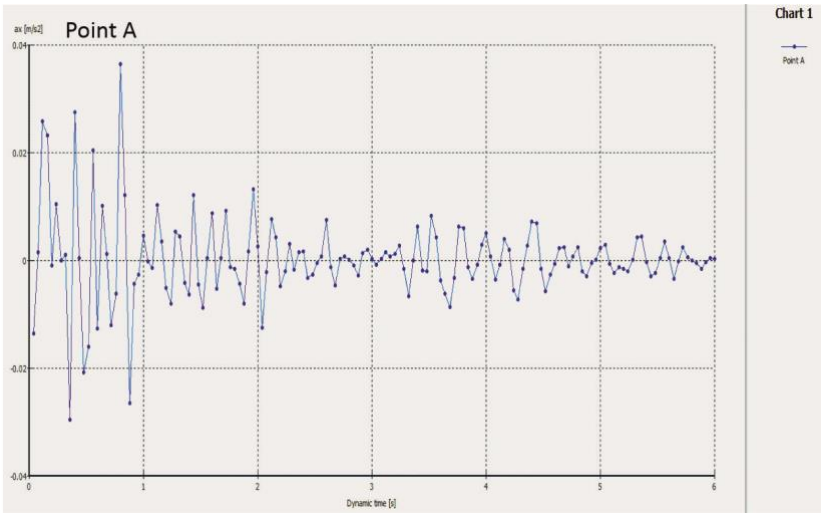

Fig. 8. Acceleration-time curve of soil with plate foundation load at surface (Point A)

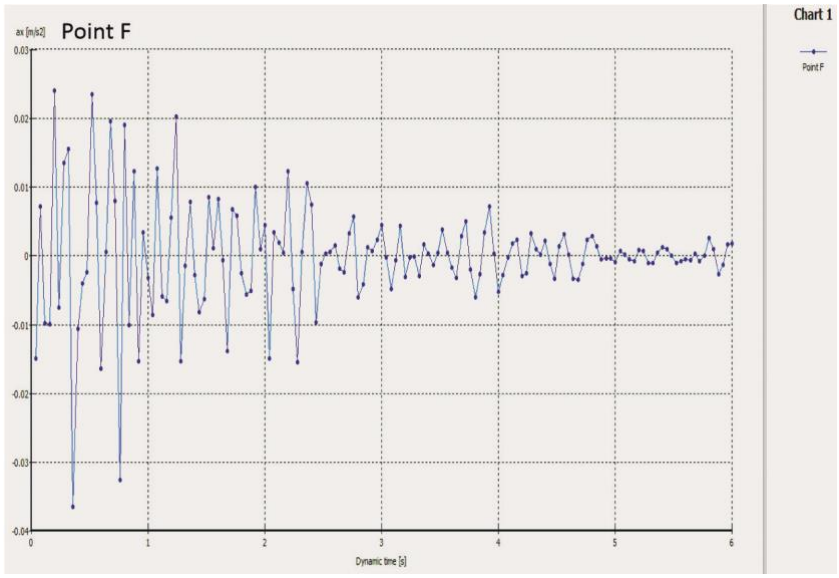

Fig. 9. Acceleration-time curve of soil with plate foundation load at bed rock (Point F)

5. Conclusions

The amplification factor (S %) to the soil in the study area is 108 % when soil is without a foundation load and 150 % when soil is with foundation load. Thus, the soil is classified as type – D (Moderate. There is no liquefaction, but subduction or landslide, so piling foundations are recommended within the area of study. As well, numerical modeling is recommended in several locations in Egypt and any other place with similar circumstances all over the world to obtain suitable areas for the foundation constructions.

Acknowledgements

I would like to express my deep thanks to all the staff members of Misr Raymond Foundations Co., all the staff members of Department of Geology, Faculty of Science, Al-Azhar University for their helping.

References

Al Azab, A.I.S., 2006. Morphological and environment of Abu Quir-Rafah coastal plain with emphasis the beach black sand, Egypt. Ph.D. Thesis, Faculity of Science, Ain Shams University.

Brimich, L., Mekkawi, M., Refai A.K., Kader, 2011. Active subsurface structures at Fayoum-Cairo district, Northern Western Desert, Egypt, as deduced from magnetic data. Contributions to Geophysics and Geodesy, 41, 329 – 351.

BSSC (Building Seismic Safety Council), 1994. Recommended provisions for seismic regulations for new buildings, 1994. Part I – Provisions, Federal Emergency Management Agency, Washington, D.C., 290.

El-Heiny, I., Enani, N., 1996. Regional Stratigraphic Interpretation Pattern of Neogene Sediments, Northern Nile Delta. Belayim Petroleum Company, 13th. Exploration and Production Conference, EGPC, Cairo, 270-290.

El-Shazly, E.M., Abdel Hady M.A., El Kassas, I.A., 1974. Geology of Sinai Peninsula from ERTS-2 Satellite Images, Remote Sensing Center, Cairo, 10.

Housner, G.W., 1952. Spectrum intensity of strong ground -motion earthquakes. In Proc. of symposium on earthquakes and blast effects on structure, Earthquake Engineering Research Institute, California, USA.

Kebeasy, R.M., 1990. Seismicity In R. Said Ed., The Geology of Egypt, S.A., A.A. Balkema Rotterdam, Brookfield, 51-59.

Kusky, T.M., Ramadan, T.M., Hassan, M.M., Gabr, S., 2011. Structural and tectonic evolution of El-Faiyum depression, North Western Desert, Egypt based on analysis of Landsat ETM+, and SRTM Data. Journal of Earth Science, 22, 75 -100.

Meneisy, M.Y.,1990. Volcanicity. In R. Said Ed., The Geology of Egypt. A.A. Balkema Rotterdam, 157-172.

Qadir, M.S., Al-Hadad, K.A., Abed, M.F., 2022. Geotechnical properties evaluation of selected reservoir sediments in Samarra Barrage and Wind Dam, Iraq. Iraqi Geological Journal, 55(2F), 138-148.

Shalal, R.S., Mahdy, M.M., Al-Ali, A.K., Hashoosh, A.M, 2022. Litho-stratigraphic mapping of the Bajalia Anticline, Missan Governorate by using digital image processing of Landsat-9 Imagery, Baghdad, Iraq. Iraqi Geological Journal, 55(2F), 114-127.

Zghair, M.M., Al-Kubaisi, M.S., Karim, H.H., 2022. Using 2D electrical resistivity imaging to evaluate soil investigations in Palm Towers Site of Al-Muthana Airport, Baghdad, Iraq. Iraqi Geological Journal, 55(2F), 128-137.